Chiroptical Properties of a Cryptophane Soluble at Neutral pH

Thierry Brotin, Nicolas Daugey, Marion Jean, Nicolas Vanthuyne, Thierry Buffeteau

Chiroptical Properties of a Cryptophane Soluble at Neutral pH

Thierry Brotin,*[a] Nicolas Daugey,[b] Marion Jean,[c] Nicolas Vanthuyne,[c] Thierry Buffeteau*[b]

[a] University Claude Bernard Lyon 1, ENS de Lyon, CNRS, UMR 5182, Laboratoire de Chimie, 69342 Lyon, France

E-mail: Thierry.brotin@ens-lyon.fr

[b] University Bordeaux, CNRS, Bordeaux INP, ISM, UMR 5255, 351 Cours de la Libération, 33405 Talence, France

E-mail: thierry.buffeteau@u-bordeaux.fr

[c] Aix Marseille Univ, CNRS, Centrale Marseille, FSCM, UAR 1739, Chiropole, 13397 Marseille, France

Abstract: This article reports the synthesis of the two enantiomers of a water-soluble cryptophane **3** enabling cesium and thallium complexation at neutral or basic pH. The two enantiomers of **3** were obtained in a two steps synthesis from cryptophane **4**, a molecule decorated with three phenol groups and three other phenol groups protected by benzyl units. The two enantiomers of **4** were isolated from liquid chromatography using chiral stationary phase. The absolute configuration of the two enantiomers of **3** was determined by vibrational circular dichroism combined with theoretical calculations. Contrary to cryptophane **1** that present large spectroscopic changes upon cesium and thallium complexation, the electronic circular dichroism spectra of compound **3** exhibit moderate spectral changes suggesting that this compound cannot change the conformation of its linkers as easily as cryptophane **1**.

Introduction

Hollow molecules constitute a very important class of compounds having the ability to encapsulate atoms and molecules in the solid state, in solution as well as in the gas phase. [1] This property can be exploited to modify the chemical and physical properties of the encapsulated host, opening a wide field of possible applications such as medical imaging, pollution control and chemical reaction. [2] Thus, different chemical structures have been imagined by chemists. Among the vast catalogue of hollow molecules reported in the literature, cryptophane derivatives constitute interesting compounds because these poly-aromatic structures can bind a large range of guest molecules depending on their structures. [3] The first cryptophane (i.e. cryptophane-A) was reported by Collet and co-workers and was one of the first host molecule able to isolate the guest molecule from the bulk. [4] This property has opened the way to potential new applications, particularly with xenon as a guest. [5] Since then, many different cryptophane structures have been reported in the literature, and cryptophane complexes have been studied using a wide range of spectroscopic techniques. [3]

For almost a decade, our group has reported that cryptophane derivatives decorated with hydroxyl functions could efficiently encapsulate cesium and thallium(I) in aqueous solutions under basic conditions. [6] Cesium and thallium(I) are two toxic metallic species of primary concern that have a huge impact on human health and living systems in general. For instance, ^{137}Cs is a radioactive element that is produced in nuclear plants. Releasing of this element into nature (Chernobyl in 1986, Fukushima in 2011) poses a major threat for living systems. [7] On the other hand, thallium(I) is considered the most toxic metal compound, and even a small uptake of this element by living systems has a harmful effect. [8] Consequently, physical and chemical methods aimed at eliminating these two species from soil and groundwater are welcome. It is noteworthy that despite the harmful effect of thallium(I) on health, radioactive ^{201}Tl (γ, $t_{1/2}$ = 3.03 days) finds some applications in radiochemistry to image and diagnose myocardial infarction. The ability of host molecules to encapsulate thallium cation could lead to new organic interesting chelators for delivering ^{201}Tl to specific tissues. [9]

Our previous work revealed that the presence of hydroxyl functions was mandatory to sequester these two species, and that complexation efficiency increased with the number of hydroxyl functions. [6c-6e] Moreover, increasing the size of the cavity decreased the complexation efficiency. [6a,6c] Thus, the *anti*-cryptophane **1** (D_3-symmetry) decorated with six hydroxyl functions shows higher binding constants in basic solutions whereas the *anti*-cryptophane **2** (C_3-symmetry) decorated with six OCH_2COOH groups was unable to bind cesium in the same conditions (Figure S17 in reference 6e). However, the very high binding constants measured for **1** were obtained under basic conditions, which prevented most of the possible applications. The selective capture of cesium and thallium by cryptophane soluble at neutral pH led us to synthesize a cryptophane of C_3-symmetry constituted of two different hemispheres since one cyclotribenzylene (CTB) group is decorated with three hydroxyl groups and the other with three OCH_2COOH functions (cryptophane **3** in Scheme 1). [10] Isothermal Calorimetric Titration (ITC) experiments revealed that the racemic form of cryptophane **3** could bind these two cationic species at basic and neutral pH with binding constants several orders of magnitude lower than compound **1**.

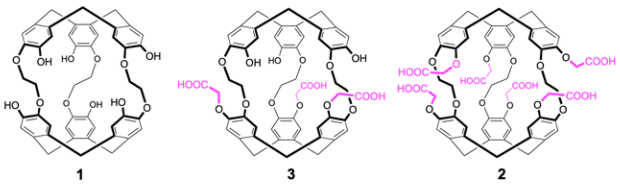

Scheme 1. Chemical structures of compounds **1**-**3**. Only a single enantiomer is shown.

Most of the cryptophane derivatives, such as cryptophanes **1**-**3**, present an inherent chirality and the separation of their enantiomers can be easily performed by HPLC techniques using chiral stationary phases. [11] In the past, chiroptical techniques have provided valuable information to characterize enantiopure cryptophane molecules and their complexes. [11] For instance, electronic circular dichroism (ECD) spectroscopy is a powerful technique to study conformational rearrangements that take place upon complexation, [12] and vibrational circular dichroism (VCD) combined with theoretical calculations allows the determination of the absolute configuration (AC) of organic molecules in solution. [13] These two chiroptical techniques have been used to thoroughly study compounds **1**-**2** and to obtain useful information upon encapsulation with various species. [6]

In this article, compound **3** has been investigated by ECD and VCD spectroscopy in order to determine the AC of the two enantiomers of **3** and the chiroptical properties of **3** during cesium and thallium encapsulation under different experimental conditions. We report the optical resolution of the cryptophane precursor **4** by HPLC and the two steps synthesis of compound **3** from this derivative. Then, VCD spectroscopy combined with density functional theory (DFT) calculations have been used to determine the AC of the two enantiomers of **3**. These two enantiomers have been investigated under different experimental conditions to reveal how the encapsulation process modifies ECD spectra during cesium and thallium complexation, giving insight into the conformational changes occurring during the binding process. Finally, these results have been compared with those obtained with compound **1**.

Results and Discussion

Synthesis and characterisation of compounds 3 and 4.

Cryptophane *anti*-**4** (Scheme 2) serves as starting material to synthesize individually the two enantiomers of the water-soluble cryptophane **3**. Compound **4** was prepared in its racemic form by a multi-steps synthesis from 3,4-dihydroxybenzaldehyde according to a procedure described in the literature. [14] Semi-preparative chiral HPLC (Chiralpak IF) was then used to separate each enantiomer of **4** as shown in Figure 1. Thus, compound $\mathbf{4}_f$ (first eluted) and $\mathbf{4}_s$ (second eluted) were obtained in fair quantity (around 250 mg) with high enantiomeric excess ee > 99.5 %, thus allowing the study of their chiroptical properties. ^{1}H and ^{13}C NMR spectra of each enantiomer of **4** are reported in Supporting Information (Figures S1-S4) and are identical to those reported previously for (*rac*)-**4**. [14] Specific Optical Rotation (SOR) values, recorded in CH_2Cl_2 at several wavelengths, are reported in Figure S5 and in Table S1. The first eluted compound gives rise to positive SOR values whereas the second eluted enantiomer gives negative SOR values. As expected for a couple of enantiomers the SOR values are of the same magnitude with opposite sign and increase as the wavelengths decrease. UV-visible and ECD spectra recorded in CH_2C_{l2} and THF are also reported in Figures S6-S7 for the two enantiomers of **4**.

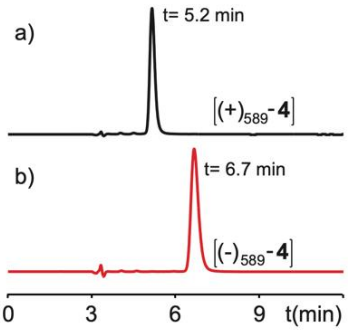

Figure 1. Separation of the two enantiomers $(+)_{589}$-**4** and $(-)_{589}$-**4** on semi-preparative HPLC (Chiralpak IF). See Experimental Section for details.

The two enantiomers of **4** were then subjected to further reactions to prepare compounds $\mathbf{3}_f$ and $\mathbf{3}_s$ (Scheme 2)**.** For instance, the first eluted enantiomer $\mathbf{4}_f$ was allowed to react with an excess of benzyl 2-bromoacetate in presence of a base to give the tris ester derivative $\mathbf{5}_f$ in 74 % yield. Then, the six benzyl groups were removed in a single step by hydrogenation in presence of Pd/C (10%) in a mixture of CH_2Cl_2 and MeOH. This gives rise to compound $\mathbf{3}_f$ with a moderate 63% yield (isolated product). The same procedure was applied to the second eluted cryptophane $\mathbf{4}_s$ to give rise to compound $\mathbf{3}_s$ in a 50% yield (isolated product). The partial solubility of compounds $\mathbf{3}_f$ and $\mathbf{3}_s$ in water explain the moderate yield of isolated compounds. ^{1}H and ^{13}C NMR spectra of compounds $\mathbf{3}_f$ and $\mathbf{3}_s$ are reported in Figures S8-S11. These spectra are identical to those reported for (*rac*)-**3**. [10]

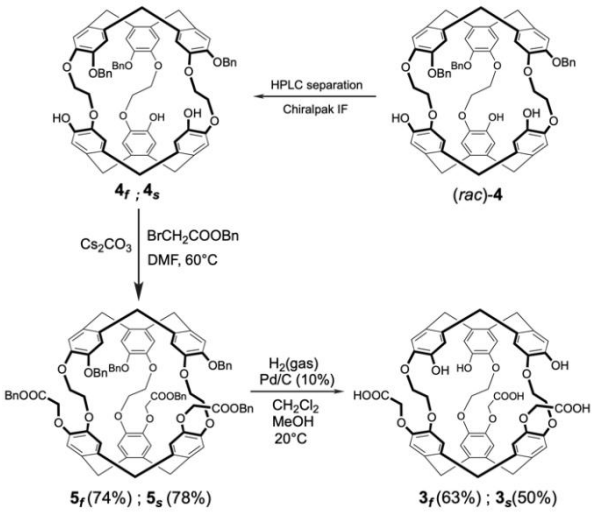

Scheme 2. Synthesis of the two enantiomers $\mathbf{3}_f$ and $\mathbf{3}_s$ from enantiopure cryptophanes $\mathbf{4}_f$ and $\mathbf{4}_s$.

VCD spectroscopy combined with DFT calculations was used to determine the absolute configuration (AC) of compounds $\mathbf{3}_f$ and $\mathbf{3}_s$. The VCD spectra of $\mathbf{3}_f$ and $\mathbf{3}_s$ are reported in Figure 2 in NaOD/D_2O solution (0.21 M, 45 μm path length) at a concentration of 30 mM for the host. These spectra show a perfect mirror image between 1750 and 1250 cm^{-1}, as expected for enantiomers. The presence of the broad band around 1600 cm^{-1} on the IR and VCD spectra (Figures 2a and 2b) confirms the carboxylate form of compound **3**. DFT calculations

(B3LYP/6-31G**) performed for the (*P*,*M*)-**3$_f$** configuration considering a *trans-trans-trans* conformation of the ethylenedioxy linkers reproduce with a good degree of confidence the experimental VCD spectrum of **3$_f$**, allowing the determination of the AC of **3** as (*P*,*M*)-**3$_f$** or (+)$_{589}$-(*P*,*M*)-**3$_f$** (Figure 2d). Herein, the sign (+)$_{589}$ refers to the sign of the SOR values recorded at 589 nm in DMSO (Table S2) and the first letter *P* refers to the CTB cap decorated with the three phenolate groups. Thus, in turn the second letter *M* refers to the CTB cap decorated with the three carboxylate groups. With these conventions, we can easily determine the AC of **4**$_f$ as (+)$_{589}$-(*M*,*P*)-**4$_f$** and **4$_s$** as (-)$_{589}$-(*P*,*M*)-**4$_s$**. Similarly, the stereo-descriptors (*M*,*M*) and (*P*,*P*) can be assigned to the intermediate derivatives **5$_f$** and **5$_s$**, respectively. For DFT calculations, both the phenol and carboxylic acid moieties have been considered in their ionized state to approximate the structure of compound **3** under basic conditions (see Experimental Section).

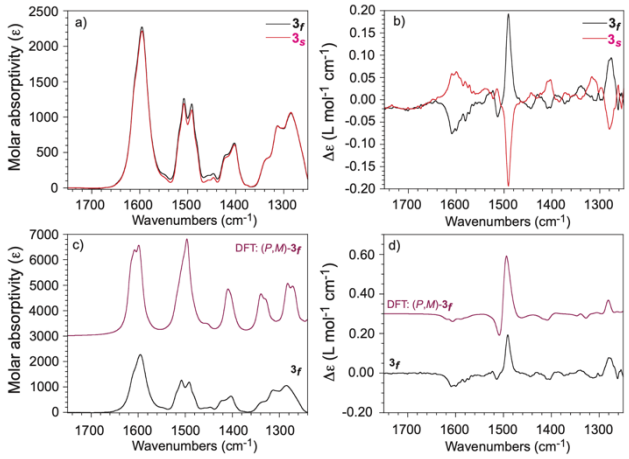

Figure 2. Experimental (a) IR and (b) VCD spectra of **3$_f$** and **3$_s$** recorded in NaOD/D_2O solution (0.21 M, 45 μm path length). The concentration of host **3** was 0.030 M. Comparison of experimental (c) IR and (d) VCD spectra of **3$_f$** (black) and predicted IR and VCD spectra calculated at the B3LYP/6.31G** level (IEFPCM=H_2O) for the *trans-trans-trans* conformation of the ethylenedioxy linkers of (*P*,*M*)-**3** derivative in its ionized form (purple).

The use of more than one chiroptical method is generally recommended to determine the AC of organic compounds. [15] Thus, Raman Optical Activity (ROA) and electronic circular dichroism (ECD) can be used as complementary tools to ascertain the AC of these enantiomers. However, in the case of compounds (*P*,*M*)-**3$_f$** and (*M*,*P*)-**3$_s$**, fluorescence signals were observed on the Raman spectra in LiOH/H_2O or NaOH/H_2O basic solutions for these two enantiomers, preventing the measure of their ROA spectra.

ECD spectroscopy has already been used to determine the AC of water-soluble cryptophanes.[11] However, the rapid AC determination by analogy with previous ECD results, also proved difficult for the two pairs of enantiomers (**4$_f$**, **4$_s$**) and (**3$_f$**, **3$_s$**). The ECD and UV-visible spectra of compounds (*M*,*P*)-**4$_f$** and (*P*,*M*)-**4$_s$** recorded in CH_2Cl_2 shows only the two symmetry-forbidden ^1L_a (~ 220-260 nm) and ^1L_b (~ 260-310 nm) transitions (Platt's notation). [16] In THF, the spectral window can be slightly extended to 210 nm revealing, at least partially, the symmetry-allowed ^1B_b transition (< 220 nm). Unfortunately, in the case of compounds (*M*,*P*)-**4$_f$** and (*P*,*M*)-**4$_s$**, the simple look of the ECD spectra is not sufficient to ascertain their AC, contrary to other cryptophanes already reported in the literature. [11] Here, the Cotton bands of ^1L_a transitions (~220-260 nm) that are typically exploited to determine cryptophane AC do not exhibit the classic positive-negative or negative-positive bisignate that is usually observed in the vast majority of cryptophane derivatives.

On the other hand, the study of the ECD spectra of compounds **3$_f$** and **3$_s$** in deionized water can be helpful in the AC determination of these compounds (Figure S12). Indeed, compounds **3$_f$** and **3$_s$** display in ^1L_a region (220-260 nm) of the ECD spectra the negative-positive and positive-negative bisignate signals, respectively. Based on the sign of this bisignate signal and by analogy with previous results, [11] it is possible to propose the chemical structures shown in Scheme 3 for compound **3$_f$** and **3$_s$**. These results are in agreement with those obtained by VCD spectroscopy.

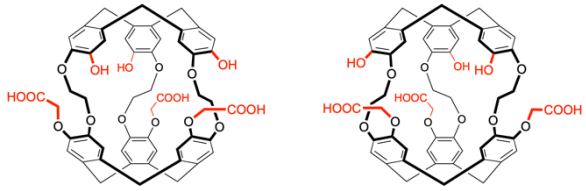

Scheme 3. Assignment of the stereo-descriptors of compounds **3$_f$** and **3$_s$**. The first stereo-descriptor refers to the CTB ring decorated with the three hydroxyl functions.

Finally, a more rigorous but time-consuming approach using TD-DFT calculations of the ECD spectrum of **3$_f$** in its ionized form can also confirm the AC of this compound. As shown in Figure S13, TD-DFT calculations (CAM-B3LYP/6-31G**) performed for the (*P*,*M*)-**3$_f$** configuration considering a *trans-trans-trans* conformation of the ethylenedioxy linkers reproduce fairly well the experimental ECD spectrum of **3$_f$**.

Conformational study

ECD spectroscopy is a chiroptical technique which gives valuable information to study conformational changes in solution. Thus, ECD spectra can be useful for assessing host-**3** behavior in aqueous solution. For example, the conformation adopted by the three linkers has a significant impact on cavity size, which in turn plays a key role in the ability of the host molecule to accommodate guest molecules. Knowledge of linker conformation is therefore a prerequisite for a better understanding of their binding properties. The high-energy region (220 nm) of the ECD spectrum is extremely useful for this purpose. [11] The Cotton band observed in this region (only partially resolved in our conditions) can be assigned to the symmetry allowed ^1B_b transitions of the six benzene chromophores. The change in intensity of this Cotton band according to experimental conditions can be exploited to shed light on the conformation of the three ethylenedioxy linkers. [17] Indeed, the study of several cryptophane allowed us to establish clear correlation between the intensity of this band and the

conformation adopted by the three linkers. Thus, a preferential *trans* conformation of the three linkers coincides with an increase in intensity of this ECD band. On the other hand, a reduction in the intensity of this band implies a conformational change of the linker into preferential *gauche* conformation. [6c-6e]

This effect can be illustrated more clearly by comparing the ECD spectra of different cryptophane hosts in LiOH/H_2O (0.1 M) (no guests except water or gas molecules can enter the cavity) and in a LiOH/H_2O (0.1 M) solution saturated in $CHCl_3$ (Figures 3a-c). Here, the presence of a large guest molecule ($CHCl_3$, V_{vdw} = 72 Å^3) in the host cavities forces the linker to increase the cavity size, leading the three linkers to adopt a *trans* conformation. For hosts **1** and **6**, $CHCl_3$ encapsulation results in an increase in intensity of the Cotton band located at 220 nm. For instance, $\Delta\varepsilon$ values of -151 and -17 were measured for $CHCl_3$@(*M*,*M*)-**1** and empty (*M*,*M*)-**1**, respectively. [17b] The same trend was observed for host (*M*,*M*)-**6** and $\Delta\varepsilon$ values of -187 and -95 were measured for $CHCl_3$@(*M*,*M*)-**6** and empty (*M*,*M*)-**6**, respectively. [17a] In LiOH/H_2O (0.1 M), the sharp decrease in intensity observed for this Cotton band suggests a conformational change of the linkers towards a preferred *gauche* conformation, leading to a reduction in cavity size of the *empty* cryptophanes. It is interesting to note that such conformational change does not takes place with host (*M*,*P*)-$\mathbf{3_s}$ as shown in Figure 3a, the three linkers adopting preferentially a *trans* conformation in LiOH/H_2O (0.1 M) and LiOH/H_2O (0.1 M) solutions saturated in $CHCl_3$. Indeed, at 220 nm, $\Delta\varepsilon$ values of -233 and -185 were measured for $CHCl_3$@(*M*,*P*)-$\mathbf{3_s}$ and empty (*M*,*P*)-$\mathbf{3_s}$, respectively. It's worth mentioning that these findings justify our choice of an all-*trans* conformation of linkers to perform DFT calculations of VCD spectra.

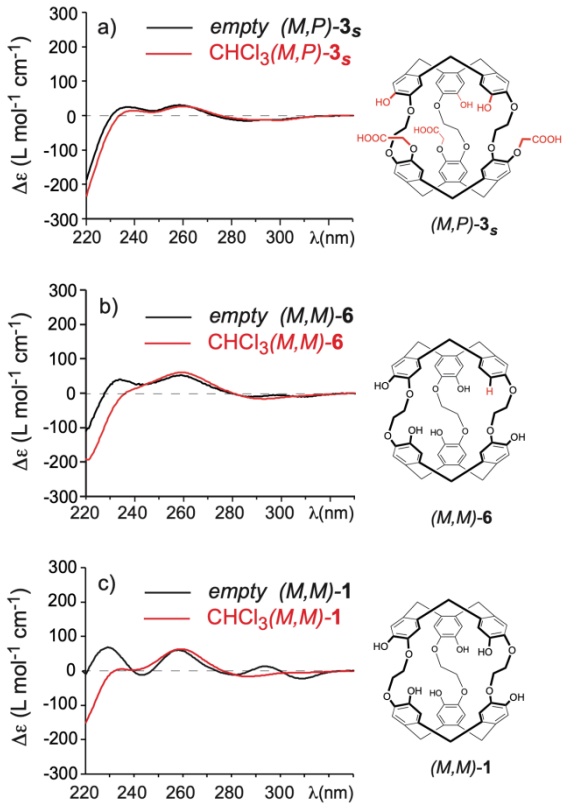

Figure 3. a) ECD spectra of compound (*M*,*P*)-**3** recorded in LiOH/H_2O (0.1 M) (black, c = 9.1 × 10^{-5} M) and in saturated $CHCl_3$/LiOH/H_2O (0.1 M) solution (red, c = 1.09 × 10^{-4} M). b) ECD spectra of compound (*M*,*M*)-**6** recorded in LiOH/H_2O (0.1 M) (black spectrum) and in saturated $CHCl_3$/LiOH/H_2O (0.1 M) solution (red spectrum). c) ECD spectra of compound (*M*,*M*)-**1** recorded in LiOH/H_2O (0.1 M) (black spectrum) and in saturated $CHCl_3$/LiOH/H_2O (0.1 M) solution (red spectrum).

Cesium and Thallium complexation by (*M*,*P*)-$\mathbf{3_S}$.

Since ECD spectra of (*P*,*M*)-$\mathbf{3_f}$ and (*M*,*P*)-$\mathbf{3_s}$ are different in pure water and in LiOH/H_2O (0.1 M) (Figure S12), we decided to examine the complexation of thallium and cesium under these two experimental conditions. However, as the addition of CsOH or TlOAc to a solution of (*P*,*M*)-$\mathbf{3_f}$ and (*M*,*P*)-$\mathbf{3_s}$ can slightly alter the pH of the solution, deionized water was replaced by Hepes buffer to keep the pH constant around 7.0. The presence of this buffer has only a small effect on the ECD spectrum of (*P*,*M*)-$\mathbf{3_f}$ as shown in Figure S14.

Introduction of 1 equivalent of CsOH to a solution of (*M*,*P*)-$\mathbf{3_s}$ in Hepes buffer (pH = 7.09) did not affect the ECD spectrum in a significant manner. Increasing the amount of cesium hydroxide up to 8 equivalents into the solution also resulted in the absence of spectral modifications (Figures S15 a-b). It is noteworthy that in these conditions host-**3** shows low affinity for CsOH and a weak binding constant K = 640 M^{-1} at neutral pH (ΔG^0 = - 3.9 kcal/mol, 298 K) has been previously measured by isothermal calorimetry titration. [10] Under this pH condition, coulombic interactions do not contribute to stabilizing the Cs^+@**3** complex, since the three phenol groups mainly exist in their OH form. Figure S15a also reveals that under these conditions Cs^+ complexation is not followed by a conformational change. Thus, an all-*trans* conformation of the linkers seems to be favored under these conditions in the absence or presence of Cs^+ in the cavity. Here, a comparison with host **1** cannot be done since this compound is not soluble at neutral pH.

Replacing CsOH by TlOAc resulted in notable modifications of the ECD spectra, in particular for the Cotton bands of the ^1L_b transition (~ 260-310 nm), as shown in Figure S15c. In addition, upon addition of 1 to 8 equivalents of a TlOAc solution, a reduction by nearly 50 % of the intensity of Cotton band located at 220 nm can be observed (Figure S15d). Taken together, these results suggest a stronger host-guest interaction and more extensive conformational changes than those observed in the case of Cs^+. These results agree well with the stronger interaction that exists between host-**3** and Tl^+ at neutral pH, K = 5750 M^{-1} (ΔG^0 = - 5.1 kcal/mol, 298 K) as determined previously by ITC experiments. [10]

In LiOH/H_2O (0.1 M) both Cs^+ and Tl^+ cations show higher affinity for (*M*,*P*)-$\mathbf{3_s}$ and binding constants K = 11000 M^{-1} and K = 4.2 × 10^5 M^{-1} have been measured by ITC at 298 K, respectively. [10] At this pH, full deprotonation of the three phenolate takes place and the coulombic interactions contribute in a significant way to the stabilization of the two complexes. In the case of the thallium cation, DFT calculations performed on a cryptophane congener of **3** have shown that the strong negative electrostatic and orbital interaction terms, with a non-negligible charge-transfer between Tl^+ and the host molecule contribute to the stabilization of the thallium-cryptophane complexes. [6b] It is

noteworthy that these association constants remain several orders of magnitude weaker than those observed with host **1** under the same experimental conditions. Indeed, K = 2.7 × 10^9 M^{-1} and K = 5.0 × 10^{10} M^{-1} have been measured for the Cs^+@**1** and the Tl^+@**1** complexes, respectively, in LiOH/ H_2O (0.1 M) at 298 K. [6c]

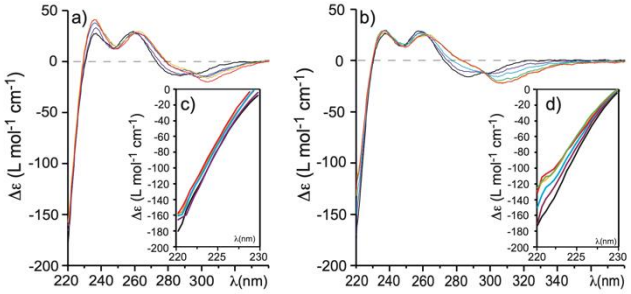

Figure 4. ECD spectra of compound (*M*,*P*)-$\mathbf{3_s}$ recorded in LiOH/H_2O (0.1 M) at 293 K. a): in presence of CsOH. Host concentration c = 3.40 × 10^{-5} M with 0 (black), 1 (purple), 2 (blue), 3 (orange) and 4 (red) equivalents of CsOH. b): in presence of TlOAc. Host concentration c = 3.50 × 10^{-5} M with 0 (black), 0.25 (purple), 0.5 (blue), 1 (green), 2 (orange) and 4 equivalents (red) of TlOAc.

It's worth noting that in LiOH/H_2O (0.1 M), the spectral modifications observed on the ECD spectra of the (*M*,*P*)-$\mathbf{3_s}$ derivative with the addition of CsOH are more important than those observed in presence of the Hepes buffer, as shown in Figure 4a. The ^1L_b region of the spectrum is the most affected upon addition of an excess of a CsOH solution and a bathochromic shift of the ECD spectra is observed. A similar behavior occurs by replacing CsOH by TlOAc but the spectral modifications appear at lower concentration of TlOAc (Figure 4b). Clear spectral changes can be observed at concentration as low as 0.25 equivalent of TlOAc. However, for the two cations, the ECD spectral modifications in the high-energy region of the spectra remain lower than those observed with host **1** under the same experimental conditions. [6c,6e]

The moderate spectral modifications observed probably results from the dissymmetrical structure of host **3** leading to preferential interactions of the two cations within the cavity of **3**. Indeed, in the case of Cs^+ and Tl^+ cations it seems reasonable to assume that these two species interact more strongly, via coulombic interactions, with the cyclotribenzylene (CTB) unit decorated with the three phenolate groups. On the other hand, interactions with CTB cap decorated with the carboxylate moieties seem limited because the negative charges carried by the carboxylate groups are more distant from the center of the cavity. In turn, this limits the coulombic interaction contribution between the cation and the carboxylate groups. The absence of complexation between host **2** and these two cations confirms these hypotheses. In contrast, host **1**, which has D_3 symmetry, interacts in the same way with both CTB caps, enabling it to establish stronger interactions with cesium and thallium cations resulting in greater conformational changes. [6c-6e]

Conclusion

We report in this article the synthesis of the two enantiomers of **3**, a C_3-symmetrical compound decorated with three phenol groups grafted on one CTB cap and three carboxylic acid moieties grafted on the second CTB cap. In a previous article, the racemic form of this compound has proved to bind cesium and thallium(I) cations in basic conditions as well as in neutral conditions. The goal of this article is to understand how the complexation of cesium and thallium(I) cations by the two enantiomers of **3** modifies the chiroptical properties of this cryptophane derivative.

The two enantiomers of **3** have been prepared separately in a two steps synthesis from the two enantiomers of compound **4**, the latter being obtained from HPLC separation using chiral stationary phase. The AC of the two enantiomers of **3** was determined by VCD spectroscopy combined with DFT calculations. This allowed the assignment of the AC of the two enantiomers of compounds **3** and **4**. Thus, the first eluted compound $(+)_{589}$-(*M*,*P*)-$\mathbf{4_f}$ on HPLC gives rise to the (*P*,*M*)-$\mathbf{3_f}$ enantiomer. In turn, the second eluted compound $(-)_{589}$-(*P*,*M*)-$\mathbf{4_s}$ gives the (*M*,*P*)-$\mathbf{3_s}$ enantiomer.

ECD spectra of compounds (*P*,*M*)-$\mathbf{3_f}$ and (*M*,*P*)-$\mathbf{3_s}$ were recorded under different conditions to better understand how the cesium and thallium(I) binding process induces conformational changes during complexation. Our results show that the complexation of cesium and thallium(I) leads to a moderate spectral change in the high energy region of the ECD spectra whatever the experimental conditions used. Thus, with these two cationic species, the binding process does not appear to significantly alter the conformation of the three linkers of cryptophane **3**, which explains the lower binding constants obtained for this compound with respect to those measured for cryptophane **1**. Nevertheless, cryptophane **3** allows the complexation of thallium(I) cations from aqueous solutions at neutral pH.

Experimental Section

Analytical HPLC separation of compounds (*M*,*P*)-4 and (*P*,*M*)-4: The sample was dissolved in dichloromethane, injected on the chiral column Chiralpak IF. Detection was achieved with an UV detector at 254 nm. The flow-rate was 1 ml/min. Two peaks corresponding to the two enantiomers (*M*,*P*)-$\mathbf{4_f}$ and (*P*,*M*)-$\mathbf{4_s}$ were located at 5.17 et 6.69 min, respectively.

Preparative HPLC separation of compounds (*M*,*P*)-4_f and (*P*,*M*)-4_s: 584 mg of (*rac*)-**4** were dissolved in 90 mL of EtOH/CH_2Cl_2 (50/50). Then, the two enantiomers were separated on Chiralpak IF (250 × 10 mm) using EtOH/CH_2Cl_2 (50/50) as a mobile phase (flow-rate = 5 ml/min, UV detection at 254 nm, 180 times 500 µL, every 4.8 minutes). From this experiment 250 mg of the first eluted enantiomer with ee > 99.5 % and 254 mg of the second eluted enantiomer with ee > 99.5% were collected. The enantiomeric purity of the two enantiomers was checked by analytical HPLC. ^1H and ^{13}C NMR are identical to those reported for the rac-**4** derivative. ^1H and ^{13}C NMR spectra of (*M*,*P*)-$\mathbf{4_f}$ and (*P*,*M*)-$\mathbf{4_s}$ are reported in Supporting Information (Figures S1-S4).

Synthesis of cryptophane (*P*,*M*)-3$_f$ and (*M*,*P*)-3$_s$: Bromomethylbenzylacetate (0.5 g, V = 380 μL, 21.8 mmol) was added to a mixture of compound (*M*,*P*)-**4$_f$** (0.2 g, 0.19 mmol) and cesium carbonate (0.18 g, 0.55 mmol) in DMF (6 mL). The mixture was stirred for 16 hours at 60°C under an argon atmosphere. Then, the mixture was poured in water and the product extracted was three times with CH_2Cl_2 (20 mL). The combined organic layers were washed five times with water to remove DMF and the dried over Na_2SO_4. Filtration and evaporation of the solvent under reduced pressure leaves a residue, which was purified on silica gel (CH_2Cl_2/AcOEt: 95/5 then CH_2Cl_2/AcOEt: 90/10). A second column on silica gel (same conditions) allow us to get compound (*M*,*M*)-**5$_f$** as an oil (0.39 g, 74 %), which was used directly for the next step.

A small amount of Pd/C (10%; 3 mg) was added to a stirred solution of compound (*M*,*M*)-**5$_f$** (0.37 g, 0.24 mmol) in CH_2Cl_2 (8 mL) and MeOH (8 mL). Hydrogen gas was then slowly bubbled for about one hour at room temperature. Then, the mixture was stirred for 18 hours at this temperature. The, block mixture was filtrated over celite and the celite was washed with a small amount of ethanol. NaOH/H_2O (0.5 M) was then added to the colorless solution. The aqueous phase was collected and then acidified with few drops of conc. HCl. The white precipitate was collected on a frit, washed with few mL of water and then dried in air. Finally, the solid was washed several times with Et_2O to give compound (*P*,*M*)-**3$_f$** as a colorless solid (0.15 g, 63 %).$[\alpha]_{589}$ = + 191.7 (c = 0.26, DMSO, λ = 589 nm, T = 20°C). ^{1}H NMR (300 MHz, DMSO-d_6) δ = 6.78 (m, 3H), 6.74 (m, 3H), 6.58 (m, 3H), 6.53 (m, 3H), 4.62 (m, 6H, AB_{sys}), 4.50 (d, *J* = 13.7 Hz, 3H), 4.40 (d, *J* = 13.7 Hz, 3H), 4.25-4.05 (m, 12H), 3.27 (d, *J* = 13.7 Hz, 3H), 3,14 (d, *J* = 13.7 Hz, 3H) ppm. ^{13}C NMR (75.5 MHz, DMSO-d_6) δ = 171.4 (3C), 147.1 (3C), 146.1 (3C), 145.7 (3C), 144.0 (3C), 133.6 (3C), 133.0 (3C), 132.5 (3C), 130.1 (3C), 119.5 (3C), 118.9 (3C), 117.8 (3C), 116.2 (3C), 68.3 (3C), 68.1 (3C), 65.9 (3C), 34.9 (6C) ppm. HRMS (ESI) calcd for $C_{54}H_{48}NaO_{18}$ 1007.2733; found 1007.2721.

The same procedure was applied to compound (*P*,*M*)-**4$_s$** and (*P*,*P*)-**5$_s$** to give rise to compound (*M*,*P*)-**3$_s$**. Thus (*P*,*P*)-**5$_s$** (0.37g, 78 %) was obtained from (*P*,*M*)-**4$_s$** (0.2 g, 0.19 mmol). Then, (*M*,*P*)-**3$_s$** (0.12 g, 50 %) was obtained as a colorless solid from (*P*,*P*)-**5$_s$** (0.37g, 0.24 mmol) according to the experimental procedure described above. $[\alpha]_{589}$ = - 184.1 (c = 0.26, DMSO, λ = 589 nm, T = 20°C). ^{1}H NMR (300 MHz, DMSO-d_6) δ = 6.77 (m, 3H), 6.75 (m, 3H), 6.58 (m, 3H), 6.52 (m, 3H), 4.59 (m, 6H, AB_{sys}), 4.48 (d, *J* = 13.7 Hz, 3H), 4.39 (d, *J* = 13.7 Hz, 3H), 4.25-4.05 (m, 12H), 3.27 (d, *J* = 13.7 Hz, 3H), 3,12 (d, *J* = 13.7 Hz, 3H) ppm. ^{13}C NMR (75.5 MHz, DMSO-d_6) δ = 171.3 (3C), 146.1 (3C), 145.7 (3C), 145.7 (3C), 144.0 (3C), 133.6 (3C), 133.0 (3C), 132.5 (3C), 130.0 (3C), 119.5 (3C), 118.9 (3C), 117.7 (3C), 116.2 (3C), 68.2 (3C), 68.0 (3C), 65.9 (3C), 34.9 (6C) ppm. HRMS (ESI) calcd for $C_{54}H_{48}O_{18}$ 1007.2733; found 1007.2718.

Polarimetric, UV-visible and ECD spectroscopy: Optical rotations of the two enantiomers of **3** and **4** were measured in DMSO and CH_2Cl_2, respectively, at 589, 577, 546.1, 435.8, and 365 nm using a polarimeter with a 10 cm path length cell, thermostated at 25 °C. Concentrations used for the polarimetric measurements were typically in the range 0.26 - 0.31 g/100 mL. UV-visible and ECD spectra of the two enantiomers of **3** were recorded in deionized water, Hepes buffer, LiOH/H_2O (0.1 M, 0.5 M, 1M) at 293 K. UV-visible and ECD spectra of the two enantiomers of **4** were recorded in CH_2Cl_2 and THF at 293 K. Quartz cell with a path length of 0.2 cm and 1 cm were used for the ECD and UV-visible experiments. A concentration range of 3.4×10^{-5} to 1.1×10^{-4} moles per liter were used for ECD and UV-visible experiments. The ECD spectra were recorded in the wavelength range of 220 – 400 nm with a 0.5 nm increment and a 1 s integration time. The spectra were processed with standard spectrometer software. A smoothing procedure was applied by using a third-order least-square polynomial fit when necessary.

IR and VCD measurements: The IR and VCD spectra were recorded with a FTIR spectrometer equipped with a VCD optical bench. [18] IR and VCD spectra were recorded at a resolution of 4 cm^{-1}, by coadding 50 scans and 24000 scans (8h acquisition time), respectively. Samples were held in a CaF_2 cell with a fixed path length of 45 μm. VCD spectra of **3*f*** and **3*s*** were measured in basic NaOD/D_2O (0.21 M) solutions at a concentration of 0.030 M. For comparison with predicted VCD spectrum, baseline corrections of the experimental VCD spectra were performed by subtracting the two opposite-enantiomer VCD spectra of **3** with division by two. In all experiments, the photoelastic modulator was adjusted for a maximum efficiency at 1400 cm^{-1}. Calculations were done with the standard spectrometer software, using Happ and Genzel apodization, de-Haseth phase-correction and a zero-filling factor of one.

DFT calculations: All semi-empirical and DFT calculations were carried out with Gaussian 16. [19] Preliminary conformer distribution search of (*P*,*M*)-**3$_f$** was performed at the molecular mechanics level of theory, employing MMFF94 force fields incorporated in ComputeVOA software package. All the conformers within roughly 8 kcal/mol of the lowest energy conformer were kept. Then, the hydrogen atoms of OH and COOH groups were replaced by Na and all the geometries were optimized at the semi-empirical level of theory, using PM7 Hamiltonian. These optimized geometries were then calculated at the DFT level using B3LYP functional and 6-31G** basis set with the use of IEFPCM model of solvent (H_2O). Finally, only the lowest energetic geometry for the *trans*,*trans*,*trans* conformation of the three linkers was kept to predict the IR and VCD spectra of (*P*,*M*)-**3$_f$**. Vibrational frequencies, IR and VCD intensities were calculated at the same level of theory. For comparison to experiment, the calculated frequencies were scaled by 0.975 and the calculated intensities were converted to Lorentzian bands with a full-width at half-maximum (FWHM) of 14 cm^{-1}.

TD-DFT calculations: Based on the B3LYP/6.31G** optimized geometries, the UV and ECD spectra were calculated using time dependent density functional theory (TD-DFT) with CAM-B3LYP functional and 6.31G** basis set. Calculations were performed considering 80 excited states. For comparison to experiment, calculated wavelength were scaled by 1.075 and intensities were convoluted to Gaussian bands with a full-width at half-maximum (FWHM) of 0.2 eV.

Acknowledgements

The French National Research Agency (ANR) is acknowledged for financial support of Project ANR CAORSS (ANR-21-CE29-0006-01).

Conflict of Interests

The authors declare no conflict of interest.

Data Availability Statement

The data that support the findings of this study are available in the supplementary material of this article.

Keywords: Cryptophane • Molecular recognition • Chirality • VCD • Thallium

[1] a) M. Yoshizawa, M. Tamura, M. Fujita, *Science*, **2006**, *312*, 251-254; b) G. Zhang et M. Mastalerz, *Chem. Soc. Rev.* **2014**, *43*, 1934-1947; c) G. Montà-González, F. Sancenón, R. Martínez-Máñez, V. Martí-Centelles, *Chem. Rev.* **2022**, *122*, 13636-13708; d) F. Beuerle, B. Gole, *Angew. Chem. Int. Ed.* **2018**, *57*, 4850-4878; e) C. A. Schalley, T. Martín, U. Obst, J. Rebek, *J. Am. Chem. Soc.* **1999**, *121*, 2133-2138.

[2] a) G. Yu, M. Jiang, F. Huang, X. Chen, *Curr. Opin. Chem. Biol.* **2021**, *61*, 19-31; b) M. Morimoto, S. M. Bierschenk, K. T. Xia, R. G. Bergman, K. N. Raymond, F. D. Toste, *Nature Catalysis* **2020**, *3*, 969-984; c) A. Pöthig, A. Casini, *Theranostics*, **2019**, *9*, 3150-3169; d) M. T. Adelba, J. C. Frias, E. García-España, H.-J. Schneider, *Chem; Soc. Rev.* **2012**, *41*, 3859-3877.

[3] T. Brotin, J.-P. Dutasta, *Chem. Rev.* **2009**, *109*, 88-130; b) A. Collet, *Tetrahedron*, **1984**, *43*, 5725-5759.

[4] J. Gabard, A. Collet, *J. Chem. Soc., Chem. Commun.* **1981**, 1137-1139.

[5] a) J. Jayapaul, L. Schröder, *Molecules*, **2020**, *25*, 4627; b) L. Schröder, *Phys. Med.* **2013**, 29, 3-16; c) P. Berthault, G. Huber, H. Desvaux, *Progr. NMR Spectrosc.* **2009**, *55*, 35-60.

[6] a) T. Brotin, P. Berthault, K. Chighine, E. Jeanneau, *ACS Omega*, **2022**, *7*, 48361-48371; b) L.-L. Chapellet, J.-P. Dognon, M. Jean, N. Vanthuyne, P. Berthault, T. Buffeteau, T. Brotin, *ChemistrySelect*, **2017**, *2*, 5292-5300; c) T. Brotin, S. Goncalves, P. Berthault, D. Cavagnat, T. Buffeteau, *J. Phys. Chem. B*, **2013**, *117*, 12593-12601; d) T. Brotin, D. Cavagnat, P. Berthault, R. Montserret, T. Buffeteau, *J. Phys. Chem. B* **2012**, *116*, 10905-10914; e) T. Brotin, R. Montserret, A. Bouchet, D. Cavagnat, M. Linares, T. Buffeteau, *J. Org. Chem.* **2012**, *77*, 1198-1201.

[7] a) H. Kato, Y. Onda, M. Teramage, *J. Environ. Radioac.* **2012**, *111*, 59-64; b) M. Chino, H. Nakayama, H. Nagai, H. Terada, G. Katata, H. Yamazawa, H. *J. Nucl. Sci. Technol.* **2011**, 48, 1129-1134.

[8] a) B. Karbowska, *Environ. Monit. Assess.* **2016**, *188*, 640; b) A. Saha, *Indian J. Occup. Environ. Med.* **2005**, *9*, 53-56; c) A. L. John Peter, T. Viraraghavan, *Environ. Int.* **2005**, *31*, 493-501; d) A. Léonard, G. B. Gerber, *Mutation Res.* **1997**, *387*, 47-53; e) V. Zitko, *Sci. Total Env*. **1975**, *4*, 185-192.

[9] G. D. Bowden, P. J. H. Scott, E. Boros, *ACS Cent. Sci.* **2023**, *9*, 2183-8195.

[10] T. Brotin, P. Berthault, D. Pitrat, J.-C. Mulatier, *J. Org. Chem.* **2020**, *85*, 9622-9630.

[11] O. Baydoun, T. Buffeteau, T. Brotin, *Chirality*, **2021**, *33*, 562-596.

[12] a) Taniguchi T. *Bull Chem Soc Jpn.* **2017**, *90*, 1005–1016; b) G. Pescitelli, L. Di Bari, N. Berova, *Chem. Soc. Rev.* **2011**, *40*, 4603-4625; c) A. Mazzanti, D. Dasarini, *WIREs Comput. Mol. Sci.* **2012**, *2*, 613-641; d) N. Berova, L. Di Bari, G. Pescitelli, *Chem. Soc. Rev.* **2007**, *36*, 914-931.

[13] a) O. Baydoun, T. Buffeteau, N. Daugey, M. Jean, N. Vanthuyne, L.-L. Chapellet, N. De Rycke, T. Brotin, *Chirality*, **2019**, *31*, 481-491; b) D. Pitrat, N. Daugey, M. Jean, N. Vanthuyne, F. Wien, L. Ducasse, N. Calin, T. Buffeteau, T. Brotin, *J. Phys. Chem. B* **2016**, *120*, 12650-12659; c) T. Brotin, D. Cavagnat, et T. Buffeteau, *J. Phys. Chem. A* **2008**, *112*, 8464-8470; d) T. Brotin, D. Cavagnat, J.-P. Dutasta, T. Buffeteau, *J. Am. Chem. Soc.* **2006**, *128*, 5533-5540.

[14] T. Brotin, E. Jeanneau, P. Berthault, E. Léonce, D. Pitrat, J.-C. Mulatier, *J. Org. Chem.* **2018**, *83*, 14465-14471.

[15] P. L. Polavarapu, *Chirality*, **2008**, *20*, 664-672.

[16] J. R. Platt, *J. Chem.; Phys.* **1949**, *17*, 484-495.

[17] a) A. Bouchet, T. Brotin, M. Linares, H. Ågren, D. Cavagnat, T. Buffeteau, *J. Org. Chem.*, **2011**, *76*, 1372-1383; b) A. Bouchet, T. Brotin, D. Cavagnat, T. Buffeteau, *Chem. Eur. J.*, **2010**, *16*, 4507-4518.

[18] T. Buffeteau, F. Lagugné-Labarthet, C. Sourrisseau, *Appl. Spectrosc.* **2005**, *59*, 732-745.

[19] M. J. Frisch, G. W. Trucks, H. B. Schlegel, G. E. Scuseria, M. A. Robb, J. R. Cheeseman, G. Scalmani, V. Barone, G. A. Petersson et al. Gaussian 16, Revision B.01; Gaussian, Inc.: Wallingford CT. M. J. Frisch, G. W. Trucks, H. B. Schlegel, G. E. Scuseria, M. A. Robb, J. R. Cheeseman, G. Scalmani, V. Barone, G. A. Petersson, H. Nakatsuji, X. Li, M. Caricato, A. V. Marenich, J. Bloino, B. G. Janesko, R. Gomperts, B. Mennucci, H. P. Hratchian, J. V. Ortiz, A. F. Izmaylov, J. L. Sonnenberg, D. Williams-Young, F. Ding, F. Lipparini, F. Egidi, J. Goings, B. Peng, A. Petrone, T. Henderson, D. Ranasinghe, V. G. Zakrzewski, J. Gao, N. Rega, G. Zheng, W. Liang, M. Hada, M. Ehara, K. Toyota, R. Fukuda, J. Hasegawa, M. Ishida, T. Nakajima, Y. Honda, O. Kitao, H. Nakai, T. Vreven, K. Throssell, J. A. Jr. Montgomery, J. E. Peralta, F. Ogliaro, M. J. Bearpark, J. J. Heyd, E. N. Brothers, K. N. Kudin, V. N. Staroverov, T. A. Keith, R. Kobayashi, J. Normand, K. Raghavachari, A. P. Rendell, J. C. Burant, S. S. Iyengar, J. Tomasi, M. Cossi, J. M. Millam, M. Klene, C. Adamo, R. Cammi, J. W. Ochterski, R. L. Martin, K. Morokuma, O. Farkas, J. B. Foresman, D. J. Fox

Entry for the Table of Contents

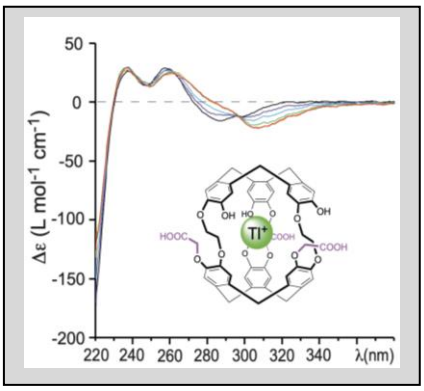

Insert text for Table of Contents here. The anti-cryptophane-**3** derivative sequesters cesium and thallium cations at neutral pH or in LiOH/H_2O solution. The two enantiomers of compound **3** were synthesized and their absolute configuration determined by VCD spectroscopy combined with DFT calculations. The ability of cesium and thallium cations to induce conformational changes was assessed by ECD spectroscopy.